Linking single particle rearrangements to delayed collapse times in transient depletion gels

2006 J. Phys.: Condens. Matter 18 11531

(http://iopscience.iop.org/0953-8984/18/50/009)

INSTITUTE OF PHYSICS PUBLISHING JOURNAL OF PHYSICS: CONDENSED MATTER

J. Phys.: Condens. Matter **18** (2006) 11531–11550 doi:10.1088/0953-8984/18/50/009

Linking single particle rearrangements to delayed collapse times in transient depletion gels

V Gopalakrishnan, K S Schweizer and C F Zukoski[1]

Departments of Chemical & Biomolecular Engineering and Materials Science & Engineering, University of Illinois, Urbana, IL 61801, USA

E-mail: czukoski@uiuc.edu

Received 18 July 2006, in final form 1 November 2006
Published 27 November 2006
Online at stacks.iop.org/JPhysCM/18/11531

Abstract

Weak depletion gels with particle radii of ∼200–500 nm have been reported to display a time-dependent settling behaviour where an initially space spanning gel displays a catastrophic collapse after a characteristic period of time, defined as the delay time. Several experiments suggest that thermally activated particle rearrangements promote macroscopic gel coarsening, which ultimately triggers the rapid collapse. The delay time is found to be a sensitive function of the colloid volume fraction and polymer concentration. We have performed systematic experiments on the silica–decalin–polystyrene depletion system to explore how colloid volume fraction, polymer concentration, particle radius and ratio of polymer radius of gyration to particle radius influence the delayed collapse time of transient gels. We employ a recently developed activated barrier-hopping theory to make predictions of the timescales over which colloids can escape localized states as a function of system parameters. Our study shows that, within experimental uncertainty, delay times follow an exponential dependence on a composite variable that is a function of the three controllable system variables, which is very similar to that predicted for the thermally activated local rearrangement timescales. This provides support for the hypothesis that thermally activated particle motions are a rate-limiting step in determining the timescale for the initiation of catastrophic collapse of transient gels. In addition, the model explains why transient gel formation is found to be absent in weak depletion gels as particle sizes are reduced.

1. Introduction

Gelled suspensions represent a class of soft materials that have wide applications [1]. Particulate gels are composed of colloidal particles that are localized by inter-particle attractive

[1] Author to whom any correspondence should be addressed.

interactions modulated by volume-exclusion-driven crowding effects. The resulting slow diffusion leads to long relaxation times and solid-like elastic behaviour [2]. Material properties can be controlled by system parameters such as the range and strength of inter-particle attractions, colloid sizes and volume fraction, solvent dielectric properties and external forces.

One method of triggering particle aggregation that has seen extensive study involves the addition of non-adsorbing polymer that induces an attractive depletion force of entropic origin between colloids [3]. Aggregation occurs when the depletion attraction overwhelms the random thermal forces that drive long range diffusion. The strength and range of the depletion attraction is controlled by the concentration and molecular weight (or radius of gyration) of the polymeric additives. While a variety of phase transformations are observed in depletion systems, here we are interested in the formation of gels that readily occur when the ratio of the polymer radius of gyration, R_g, relative to the particle radius, R, is less than $\sim$0.1. A significant degree of success has been recently achieved in understanding how depletion interactions alter the suspension microstructure under equilibrium conditions and the mechanical responses of these suspensions [4–11]. At the gel point, dense percolating clusters are formed and the microstructure and mechanical properties of the suspensions have been determined in the linear viscoelastic regime [3, 9].

Most studies have focused on regimes in which particles are sufficiently strongly localized that the material properties are essentially time invariant on experimental timescales. However, a number of systems exist whose properties are determined by their age in addition to other parameters. Thixotropic suspensions are the most often observed class of materials with time-dependent properties [1]. From an industrial perspective, understanding how sample age affects properties is critical to determining the durability or shelf-life of products.

An interesting example of time-dependent behaviour has been reported by Poon and co-workers [12], where a form of delayed settling is observed in weakly aggregated depletion gels, defined as 'transient gels'. In these systems, upon preparation, the gels form a structure that is space filling. However, after a characteristic period of time, defined as the delay time, the gel catastrophically collapses, resulting in a consolidated sediment at the bottom of the vial. Delay times are reported to increase strongly with increasing polymer concentration and colloid volume fraction. Delayed settling is associated with the network losing its ability to sustain gravitational stresses after a period of time. Direct observation of the gel with dark field imaging techniques [12] reveals that at about the time of collapse 'streamers' and large scale fissures appear, that facilitate the up-flow of the solvent, thereby accelerating gel collapse. These observations make it apparent that transient gels are subject to a variety of restructuring mechanisms that are potentially governed by a number of parameters. Interestingly, delayed settling has also been reported in several other colloidal systems [13–16], suggesting that a common underlying physics may govern the various processes that eventually trigger gel collapse.

Since particles experience relatively weak attractions in transient gels, thermal fluctuations are capable of breaking the 'physical bonds', providing opportunities for particles to 'de-localize' and re-arrange their positions on experimentally accessible timescales. Confocal microscopy experiments [13] have provided visual evidence of random bond breakage in transient gels. Similar evidence has been found in simulations of high volume fraction particle gels [17]. Dynamic light-scattering (DLS) experiments [18, 19], which probe delay times up to $\sim 10^3$–10^4 s, report a long time exponential decay in the correlation function, suggesting that particles diffuse out of localized states given a sufficient amount of time. Thus, thermal fluctuations provide a mechanism by which particles rearrange their positions, leading, over time, to macroscopic structural changes and ultimately a collapse of the gel network. Poon and co-workers [12] discuss possible mechanisms by which these thermally activated

rearrangements can result in a more compact arrangement of particles. These rearrangements would result in the opening up of larger void spaces and therefore increased gel permeability for settling. The resulting faster solvent up-flow would then be expected to enhance bond-breakage rates, thereby accelerating gel breakup and coarsening the gel structure. Ultimately, the gel is weakened to a point that it is unable to support its own weight and this finally leads to catastrophic gel collapse.

Here we pursue a quantitative test of the idea that thermal-fluctuation-induced bond breakage and single particle activated hopping is the rate-limiting step in determining the delay time for gel collapse. A systematic study of how the colloid volume fraction, ϕ, polymer concentration, polymer radius of gyration, R_g, and particle size, R, influence the experimental delay times is performed. The recently proposed barrier-hopping theory [20] incorporates activated dynamics in a manner that builds on the naive mode-coupling theory (NMCT) [11, 21], which is a simplified version of the ideal mode-coupling theory (MCT) [22]. This theory makes predictions for single particle 'de-localization' times in structurally arrested systems [20, 23] and gel boundaries [11], which have been shown to accurately capture experimental observations of both particle localization (gel formation) and mechanical properties (elastic modulus in the linear viscoelastic regime). Using a non-equilibrium free energy construct to describe the resistance associated with inter-particle depletion attractions to long time diffusion, the theory can predict barrier hopping or ergodicity restoring timescales in depletion gels [23]. As demonstrated in the following sections, experimentally observed delay times for macroscopic gel collapse display a roughly universal behaviour, that is similar to the predictions of single particle hopping times. This lends support to the hypothesis that elementary bond-breakage events are the rate-limiting steps that trigger gel collapse.

A brief review of the activated barrier-hopping theory is given in section 2. In section 3, we discuss the experimental techniques employed in the study. Section 4 presents our experimental findings, where we find that, in addition to the volume fraction and polymer concentration [12, 13], delay times are also dependent on the particle size and the ratio R_g/R. To fully understand these observations the influence of weak residual attractions arising from a small mismatch in the refractive indices of the solvent and colloid is discussed. In section 5, we demonstrate that for a given particle size delay times follow a polymer concentration, volume fraction and polymer radius of gyration scaling as predicted by the activated barrier-hopping theory for single particle de-localization events [23]. In addition, particles of different sizes are found to fall into different 'classes' due to the influence of gravitational stresses on the delayed collapse phenomenon. Section 6 presents the conclusions.

2. Activated barrier-hopping theory

In this section we briefly review the NMCT and activated hopping theories for spherical particle suspensions. All technical details have been given in exhaustive detail in prior publications [11, 20, 23, 24]. The dynamic order parameter is the scalar displacement of a colloid from its initial position, $r(t)$, which obeys a closed non-linear stochastic Langevin equation of motion that in the overdamped limit is given by [20, 24]

$$\zeta_s \frac{\partial r(t)}{\partial t} = -\frac{\partial F(r(t))}{\partial r(t)} + \delta f(t) \tag{1}$$

where $\zeta_s = \frac{g(2R)k_BT}{D_0}$ is a short time friction constant, k_B is Boltzmann's constant, T is temperature, D_0 is the Stokes–Einstein diffusion coefficient at infinite dilution and $g(2R)$ is the contact value of the radial distribution function. The random thermal force satisfies the standard white noise fluctuation–dissipation relation $\langle \delta f(0)\delta f(t)\rangle = 2k_BT\zeta_s\delta(t)$. The key

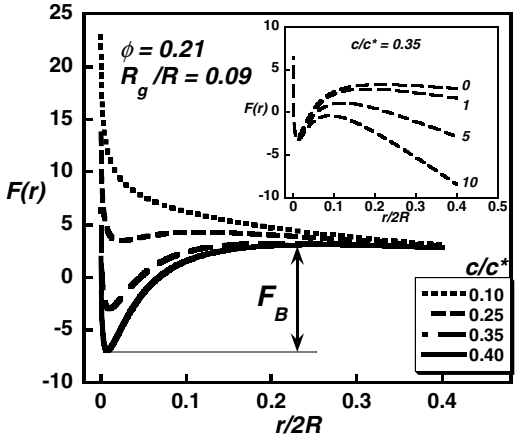

Figure 1. Plot of the non-equilibrium free energy [23] (units of $k_B T$) as a function of the normalized particle displacement for $\phi = 0.21$ and $R_g/R = 0.09$. The location of the minimum represents the localization length, and the barrier (F_B) quantifies the resistance to long time diffusion. The inset shows how $F(r)$ is modified by an applied stress at a given polymer concentration [28]. The stress values, σ, are displayed next to the respective plots (in units of $k_B T/(8R^3)$).

quantity is the nonequilibrium or effective free energy, $F(r(t))$, which quantifies within a local equilibrium, dynamic density functional framework the effect of surrounding particles on the tagged particle dynamics [24]. It can be explicitly expressed in terms of $r(t)$ and the colloid equilibrium collective structure factor [20, 24] computable from the polymer reference interaction site model (PRISM) theory for polymer-particle suspensions. The PRISM theory [25] has been shown to accurately predict the colloidal structure factors of well characterized silica–decalin–polystyrene suspensions under equilibrium conditions [10]. This allows quantitative, no-adjustable-parameter dynamical predictions to be made for colloid–polymer suspensions at both the ideal MCT and the activated barrier-hopping theory levels. Solution of equation (1) in the absence of noise yields the NMCT self-consistent equation for the long time limit of the particle displacement or localization length [11, 21]. The system conditions (colloid volume fraction, polymer concentration etc) that signal the first localized solution define the ideal gel transition. The zero-frequency elastic shear modulus G' can be immediately computed from the standard Green–Kubo formula [4, 8, 11].

Within the activated barrier-hopping theory [20, 24], the ideal MCT non-ergodicity transition signals a qualitative change in the nonequilibrium free energy to a form that involves a localization well and a barrier (as illustrated in figure 1), and thus a crossover to activated dynamics. The mean first passage, or barrier-hopping time, τ_{HOP}, can be computed from the high friction overdamped (diffusive barrier crossing) version of Kramers' theory [26]

$$\frac{\tau_{HOP}}{\tau_0} = \frac{2\pi g(2R)}{\sqrt{\tilde{K}_O \tilde{K}_B}} \exp\left(\frac{F_B}{k_B T}\right) \tag{2}$$

where $g(2R)$ is the colloid contact value computed from PRISM theory, $\tau_0 = R^2/D_0$ is the elementary Brownian diffusion time, F_B is the barrier height and $\tilde{K}_O$ and $\tilde{K}_B$ are the absolute magnitudes of the well and barrier harmonic curvatures in units of $k_B T/(2R)^2$, respectively.

Kobelev and Schweizer have extended the above theory to treat the effect of external stress in colloidal glasses and gels [27–29]. When an external mechanical force is applied to a suspension, it distorts the effective free energy and reduces the barrier which leads to

modulus softening, enhanced delocalization and a reduced barrier-hopping time. Specifically, a constant applied stress is modelled as inducing a constant force f on the tagged particle, which is proportional to the applied stress times the cross-sectional area of a particle [27]. The concept is illustrated in the inset plot of figure 1, and the details of the numerical implementation are given in [27–29].

3. Experimental methods

3.1. Particle synthesis

The Stober method [30] is employed to synthesize silica particles of a certain seed size. As per the technique, the base-catalysed hydrolysis of tetraethyl *ortho*-silicate (TEOS) is performed in an ethanol medium following a set recipe to obtain the desired seed size. Using the 'double-addition' process developed by Bogush and Zukoski [31], the silica seed particles are then grown to the final desired size. For the present study two distinct particle sizes were synthesized, 188 and 275 nm in radius. The final sizes are confirmed by scanning electron microscopy measurements. The 188 nm particles have a polydispersity of ∼5%, and the 275 nm particles have a polydispersity of ∼10%. Once synthesized, the ethanol solvent is boiled off and the particles are suspended in liquid octadecanol at a temperature of roughly 210 °C for a period of 6 h. This enables a dense layer of octadecyl chains to be grafted on the surface of the silica particles, that renders them hydrophobic and soluble in a number of non-polar organic solvents. As recommended by Van Helden *et al* [32], the amount of octadecanol used in the surface grafting technique is around three to five times the yield of the synthesized particles. After the grafting process, the mixture of particles and unreacted octadecanol is washed in a sufficient amount of chloroform and centrifuged to obtain a sedimented cake of the washed particles. The unreacted octadecanol is discarded in the supernatant. The wash process is repeated several (three to six) times to eliminate any traces of the unreacted octadecanol. The particles are then dried in a vacuum oven for ∼24 h to remove traces of the wash solvent. A particle density value of 1.8 g ml^{-1} was used to calculate colloid volume fractions for all suspensions.

3.2. Sample preparation

For the present study, we examine the effect of four system parameters on the time for the initiation of rapid collapse of transient gels: polymer concentration, particle radius, R, colloid volume fraction, ϕ, and size asymmetry ratio, R_g/R. The solvent used is decalin, which was purchased from the Sigma Aldrich Company. Due to the near-match of the refractive indices of decalin and silica, van der Waals attractions are minimized. However, due to the large particle sizes used in our study, these residual attractions cannot be completely ignored, and their implications are discussed later. The polymer employed is polystyrene of three molecular weights (M_w)—641 340, 96 900 and 382 100 g mol^{-1}, all of which are purchased from the Sigma Aldrich Company. Decalin serves as a near-ideal solvent for polystyrene as has been characterized by Shah *et al* [33]. Using their characterization results, the radius of gyration, R_g, for the above three polymer molecular weights is determined to be 21.1, 8.2 and 16.3 nm respectively. The first two molecular weight polymers are utilized with the 275 nm particles to study the impact of the size asymmetry ratio at constant R, i.e. $R_g/R = 0.076$ and 0.029, respectively. The third molecular weight polymer is used with the 188 nm particles corresponding to $R_g/R = 0.086$, which is nearly equal in magnitude to the $R_g/R = 0.076$ for the 275 nm particles, and hence is employed to probe the role of particle radius at a nearly

constant R_g/R. For both particle radii, the delayed-settling behaviour is studied at two distinct colloid volume fractions, $\phi \sim 0.22$ and ~ 0.27.

Samples are prepared by adding requisite amounts of stock colloidal suspension and stock polymer and the remaining volume is made up by adding decalin to obtain the desired ϕ and dimensionless polymer concentration, c/c^*, where $c^* = 3M_w/4\pi R_g^3 N_A$ is the overlap concentration that signifies the transition from the dilute to the semi-dilute region for the polymer solution and N_A is the Avogadro number.

3.3. Measurement procedure

All settling experiments are performed in a cylindrical vial with a fixed diameter of $\sim$1.2 cm. The initial sample height for all samples is 2 cm. Prior to starting the experiment, all samples are vortexed at high speeds to ensure that the sample is well mixed. However, this vortexing introduces air bubbles that are observed to have a significant influence on the settling behaviour of suspensions, similar to that reported in other studies [12, 16]. To eliminate air bubbles, we employ a gentle vortexing technique of the sample vial to force the air bubbles to the surface so that the suspension bulk is devoid of externally induced inhomogeneities. The gentle sample shaking is performed for several minutes and kept consistent for all samples. With this protocol, we are able to reproduce the delay-times to within $\sim$10–20%, an accuracy similar to that achieved by Poon and co-workers [12] in their studies of the delayed settling response of poly(methyl methacrylate) (PMMA)–polystyrene–decalin transient depletion gels. After the gentle shaking, the sample vial is immediately placed in an enclosed environment so that convective currents do not disturb the sample while under observation. As time progresses, the gel begins to sediment and the interface moves towards the bottom of the vial and a clear supernatant forms at the top. The interface of the sediment and supernatant defines the sediment height and is recorded using a non-intrusive telescopic viewfinder attached to a Vernier scale with an accuracy of $\sim$0.001 cm.

For all samples discussed here, we observe a transition from a slow settling regime to a regime where the sample collapses rapidly to form a consolidated cake at the bottom of the vial that finally compacts slowly with time. The initial slow settling is observed over a change of interface height of only 1–2 mm. This, and other factors, precludes establishing detailed quantitative trends for the initial sedimentation velocities prior to gel collapse. A typical example of the settling behaviour is shown in figure 3 for the 275 nm samples at $\phi = 0.275$ and $R_g/R = 0.076$. We terminate measurements when samples settle at rates that are slower than the initial settling rates. The final compacted volume fraction, ϕ_f, is then determined by multiplying the initial volume fraction, ϕ_0, by the ratio of the initial sample height to the final sample height. We find that defining a final settling height is only approximate as the sample continues to settle slowly for long periods of time after the final sample height has been defined. Thus we expect a significant amount of uncertainty in the determination of ϕ_f in addition to that which arises from reproducibility, and hence restrict ourselves to making qualitative conclusions from observations of ϕ_f.

4. Experimental results

Our aim is to understand the effects of increasing polymer concentration for different particle sizes, volume fractions and radii of gyration on delayed settling times. Shah *et al* [33] performed detailed measurements of the gel boundary on a similar experimental system over a volume fraction range of $\sim$0.10–0.40 for several R_g/R ratios below 0.1, with a particle radius of 50 nm. The gel boundary was defined as the first appearance of a uniform turbid phase.

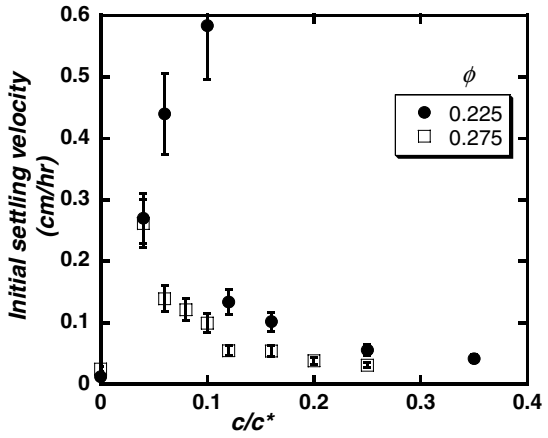

Figure 2. Initial settling velocity as a function of normalized polymer concentration for samples composed of 275 nm particles and $R_g/R = 0.076$. The behaviour of samples of 188 nm particles is identical.

For volume fractions less than 0.35, gels close to the gel boundary eventually settled to form a consolidated particle phase leaving behind a particle-free supernatant. At these particle sizes, it is visually easy to distinguish the fluid from the gel. However, as particle size increases, the silica–decalin system becomes more turbid. For the particle sizes used in our study the suspensions, both polymer free and transient gel systems appear equally turbid to the naked eye and hence the gel boundary cannot be determined by mere visual inspection.

To determine the location of the gel boundary (defined as c_{gel} at a particular ϕ), we investigated the initial settling velocity of the suspensions with increasing polymer concentration. Figure 2 shows a plot of the initial settling velocities for $R = 275$ nm and $R_g/R = 0.076$ for volume fractions of 0.225 and 0.275. For both volume fractions, an identical trend is observed. By increasing the amount of polymer in the suspension, the settling velocity increases. However, above a critical polymer concentration an apparently discontinuous drop in initial settling velocity occurs with further increases in the polymer concentration, and the initial settling velocity continues to decrease even though particles are expected to settle more rapidly with increasing strength of attraction as observed at the lower polymer concentration. This abrupt decrease in the initial settling rate indicates a transition from an equilibrium fluid phase to a state where the permeability for the up-flow of the solvent dramatically drops and inter-particle stresses are capable of supporting the gravitational forces acting on the particles.

Several studies [2, 3, 34, 35] on depletion gels demonstrate that the equilibrium fluid phase and the transient gel state are separated by a region of equilibrium cluster formation where particles aggregate to form clusters that do not form a percolating network. Recently we have studied the settling properties of these clusters in dilute suspensions, where we observe that the settling velocity of the clusters is set only by the colloid volume fraction and is independent of the polymer concentration. To a first approximation, Stokes' settling velocities for these clusters suggest their radii are $\sim 50R$ if we assume clusters of uniform sizes. If the polymer concentration is fixed and the particle volume fraction is increased, at some point the clusters percolate and settling is dramatically slowed. As the particle volume fraction is increased, the range of polymer concentrations where freely settling clusters can be observed narrows. For suspensions with volume fractions above approximately 0.20 [12], the window for equilibrium cluster formation is very small and transient gel formation occurs almost immediately above the

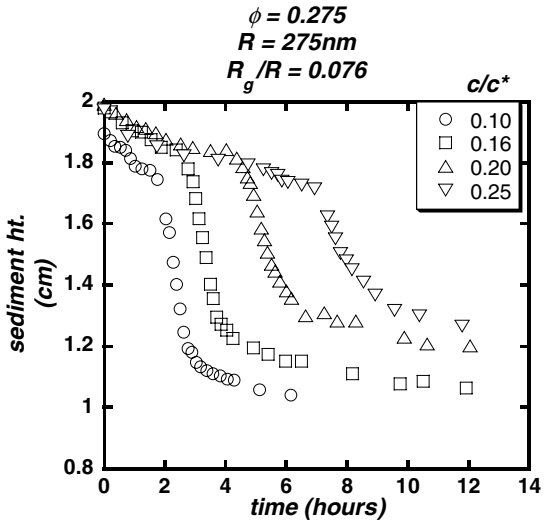

Figure 3. Sample height as a function of elapsed time. The initial sample height was kept constant at ∼2 cm for all systems studied.

equilibrium fluid phase. With further small increase in polymer concentration, transient gels are no longer observed and the gel remains stable without any evidence of settling for months.

These observations indicate that the dramatic drop in settling velocity seen in figure 2 is indicative of both cluster formation and percolation to form space-spanning gels. With increasing polymer concentration, the network strength increases, thereby increasing the net resistance to settling, and as a result the initial settling velocity decreases. The technique of figure 2 has therefore been employed to define the gel boundary at a given volume fraction as the mean of the polymer concentration values that demarcate the two initial settling velocity regimes. The gel boundary polymer concentrations for the different system parameters employed in the study are listed in table 1.

Table 1. Polymer concentrations at the transient gel boundary for the different values of colloid volume fraction, particle radius and R_g/R ratios employed in the study.

ϕ	R_g/R	R (nm)	c_{gel}/c^*
0.225	0.076	275	0.10
0.275	0.076	275	0.05
0.225	0.029	275	0.03
0.275	0.029	275	0.01
0.21	0.086	188	0.14
0.26	0.086	188	0.10

For the volume fractions and particle sizes in this study, the samples immediately above the gel boundary display a transient gel-like response, similar to what has been reported previously [12]. Shah *et al* [33] did not observe transient gels in their determination of the gel boundary for $\phi < 0.35$ (however, they do report continued slow settling), although their silica-based system is identical to ours, with the only difference being that they performed their experiments on a smaller particle radius of 50 nm. As discussed below, the absence of a transient gel phase can be attributed to the smaller particle size employed by Shah *et al* [33].

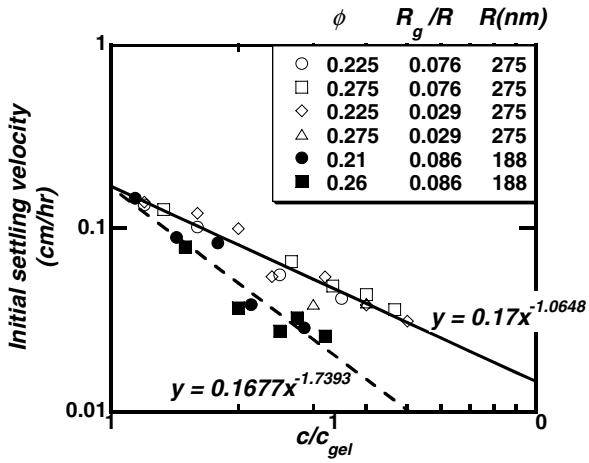

Figure 4. Initial settling velocity as a function of polymer concentration normalized to the concentration at the gel boundary for each set of conditions specified in the figure. The lines are power law fits to data for a particular particle radius.

Typical results for changes in sediment height with time are shown in figure 3 for 275 nm particles and $\phi = 0.275$, $R_g/R = 0.076$ and different values of c/c^*. In the initial slow settling regime, the settling velocity is of the order of $\sim$0.05 cm h^{-1} ($\sim$100 nm s^{-1}). After a characteristic period of time, defined as τ_{delay}, the rapid collapse regime is entered, during which the gels collapse at rates that are an order of magnitude faster than in the initial slow settling regime. At a given volume fraction, τ_{delay} increases with increasing polymer concentration. Once the sediment collapses significantly (to $\sim$ half the initial column height to an average volume fraction of $\sim 2\phi_0$), the fast settling regime again crosses over to a regime of slow gel consolidation. In this second slow settling regime, consolidation, although slow, occurs for a significant amount of time after the end of rapid collapse. Below we first discuss briefly the impact of the various system parameters on the initial settling velocity and the final compacted volume fraction, ϕ_f, and then describe in detail our observations of the delay times.

4.1. Initial settling velocity

The initial settling velocities for all the transient gel samples studied are presented in figure 4 where one can clearly distinguish the settling velocities of suspensions comprised of particles of different size. Samples composed of the 188 nm colloids settle more slowly with increasing polymer concentration than those composed of the 275 nm particles. This behaviour is consistent with the gravitational force that drives settling increasing with particle size. However, what is not expected is that for a given colloid size the initial settling velocity appears to be independent of ϕ and R_g/R.

In their model for the sedimentation of gels, Buscall and White [36] predict that under the effect of a uniform driving force the initial settling velocity of percolated networks should depend on the compressive yield stress (P_y) of the gel network. The model states that

$$u|_{t\to 0} = -\frac{(1-\phi_0)u_0}{\xi(\phi_0)}\left[1 - \frac{1}{B}\right] \tag{3}$$

$$B = \frac{\Delta\rho g \phi_0 H_0}{P_y(\phi_0)} \tag{4}$$

where $u|_{t\to 0}$ is the initial settling velocity of the network, ϕ_0 and H_0 are the initial volume

fraction and sample height of the suspension, respectively, $\Delta\rho$ is the difference in density of the particles and the solvent ($\sim$900 kg m^{-3} for our system) and g is the gravitational acceleration. $\xi(\phi_0)$, the hydrodynamic resistance due to the up-flow of the solvent, can be estimated from the Carman–Kozeny permeability [37]: $k(\phi_0) = 0.022R^2\frac{(1-\phi_0)^3}{\phi_0^2}$ since $\xi(\phi_0) \sim R^2/k(\phi_0)$, or other semi-empirical approaches. $P_y(\phi_0)$ is the compressive yield stress of the initial network. The settling velocity of the particle at infinite dilution is $u_0 = \frac{2\Delta\rho g R^2}{9\eta_s}$, where η_s is the solvent viscosity. We expect the parameters ϕ and R_g/R to have the greatest impact on $P_y(\phi_0)$ since over the range of volume fractions studied the hydrodynamic resistance is not expected to vary by a large amount. However, equation (3) becomes relatively insensitive to B when $B \geqslant 10$. Under these circumstances the initial settling velocity will be independent of the parameters that govern the compressive yield stress of the gel network.

To test if the above scenario is applicable to our study, we estimate B for our system. Channell and Zukoski [38] report that for aggregated alumina suspensions the ratio of the compressive yield stress to the shear modulus, P_y/G', is nearly constant ($\sim$10) over a wide range of volume fractions and strengths of attraction. If we assume this to hold for our depletion system as well, one can employ the relation [11] $G' = \Lambda G'_{\mathrm{NMCT}}$, where G'_{NMCT} is the prediction of the linear elastic modulus by the NMCT-PRISM theory [11] for the depletion gels and $\Lambda \sim 10^{-2}$ is a prefactor correction that accounts for the presence of dense clusters in the concentrated gel [9, 11]. From figure 1 of Kobelev and Schweizer [28] one deduces values of $G'_{\mathrm{NMCT}}(R_g/R)^2 \sim 0.5$ over a volume fraction range of $\phi = 0.20$–0.40 close to the gel boundary, i.e. $c/c_{\mathrm{gel}} \to 1$. Using the above relations, for the 275 nm particles and $R_g/R = 0.076$ and 0.029, we find $P_y \sim 0.2$ Pa ($B \sim 200$) and $\sim$1.5 ($B \sim 30$), respectively, close to the gel boundary. For the 188 nm particles and $R_g/R = 0.086$, we find $P_y \sim 0.5$ Pa ($B \sim 80$). For the 275 nm particles, at both values of R_g/R, $B \geqslant 10$ up to $c/c_{\mathrm{gel}} \sim 1.25$–2, and for the 188 nm particles we estimate $B \geqslant 10$ up to $c/c_{\mathrm{gel}} \sim 1.5$. Although there are several approximations involved, the large calculated values of B for polymer concentrations significantly above the gel boundary are consistent with the hypothesis that these samples are sufficiently weak (small P_y) that the initial settling velocity is independent of ϕ and R_g/R over the range explored in our study.

The weak dependence on polymer concentration can be attributed to the possibility that as the gel network settles, the frictional force that the gel network experiences as it slips against the walls of the vial is proportional to the attractive depletion force between the container wall and the particles at the gel network–wall interface. Again we expect this force to increase with polymer concentration and therefore slow down the initial settling rate. Since we did not perform experiments with vials of variable gel-container adhesive interactions we cannot comment in detail on the implications of such boundary conditions on the settling behaviour.

The initial settling velocities of the depletion gels in our study appear to be primarily governed by the permeability to the up-flow of the solvent. The increase in the settling velocity of the gels beyond τ_{delay} can thus be attributed to a change in this permeability that could result from structural changes driven by particle rearrangements.

Evans and Starrs [39] discuss the concept of a stress transmission length scale in transient gels, wherein at sufficiently large initial sample heights the percolated network is incapable of transmitting gravitational stresses to the bottom of the sample vial. We propose that this can also be interpreted as a sample that possesses a very small compressive yield stress relative to the applied gravitational load (in other words, a very large B). Comparing our initial sample heights (2 cm) with figure 13 of their study [39], and given the stronger gravitational force arising from a larger density difference for our system, we believe our experiments are in a regime where the sample height exceeds the stress transmission length scale.

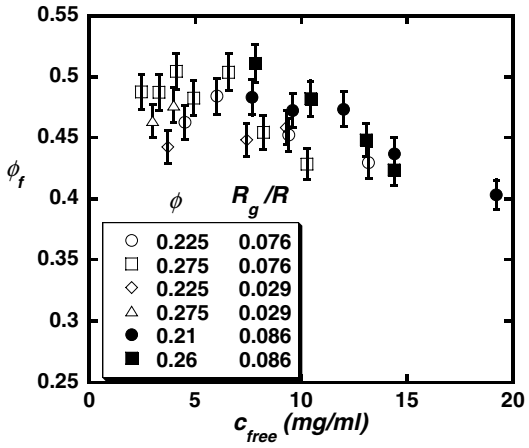

Figure 5. Final colloid volume fraction as a function of the concentration of free polymer in the suspension for all samples. The open symbols are for gels of 275 nm particles whereas the closed symbols are for 188 nm particles. The data indicates a weak dependence on polymer concentration for both particle radii.

4.2. Final volume fraction

Figure 5 plots the final volume fraction, ϕ_f, at the end of the settling process as a function of c_{free}, defined as the polymer concentration in the accessible volume of the suspension as calculated according to the free volume model of Lekkerkerker and co-workers [40]. Plotting the data in this manner enables a direct comparison with figure 2(c) in [12]. ϕ_f is defined as $\phi_0(H_0/H_f)$ where H_f is the final height of the sediment. H_f is determined when the settling velocity of the suspension has approached, or is smaller than, the initial settling velocity of the suspension (of the order of $\sim$100 nm s^{-1}), a value similar to that used previously [12]. We recognize that the suspension continues to settle slowly for a significant amount of time after the measurement of H_f, therefore making it impossible to obtain a true H_f. However, within the constraints of this definition, we observe that, over a wide range of c_{free}, ϕ_f appears fairly independent of R_g/R and R for the range of ϕ_0 employed in this study. However, ϕ_f is weakly dependent on polymer concentration. When compared to similar data on the PMMA colloid system [12] at similar particle radii (275 nm in our study and 300 nm in [12]), R_g/R ratios (0.076 in our study and $\sim$0.06 in [12]) and ϕ_0 (0.225 in our study and 0.20 in [12]), we note that in the silica–decalin system ϕ_f is larger. This appears consistent with the fact that in the silica–decalin system the gravitational forces are greater, and therefore a higher degree of compaction is achieved, resulting in a larger ϕ_f.

4.3. Delay time

The delay time, τ_{delay}, for samples composed of the 275 nm particles is shown in figure 6 as a function of c/c^*. τ_{delay} is determined from the intersection point of linear fits to the initial slow settling regime and the rapid collapse regime. As reported for PMMA depletion gels [12], at a given value of R_g/R the time required to observe the rapid gel collapse increases with ϕ. Decreasing R_g/R shifts τ_{delay} to smaller polymer concentrations, indicating that smaller R_g/R ratios move the transient gel boundary to smaller c/c^* at the same volume fractions. These observations are consistent with the NMCT-PRISM calculations [11] that predict a systematic decrease in the polymer concentration required to induce particle localization with

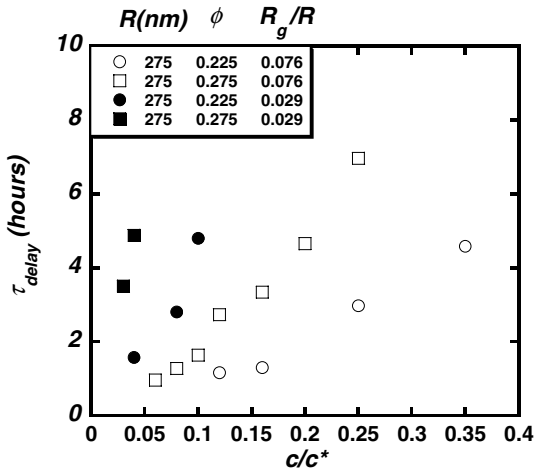

Figure 6. Delay time (in hours) for rapid collapse as a function of normalized polymer concentration for two distinct R_g/R ratios and ϕ values for $R = 275$ nm. The delay time measurements are reproducible to within a ∼10–20% accuracy. By reducing R_g/R, the polymer concentration required for transient gels to collapse at a given τ_{delay} shifts to smaller values.

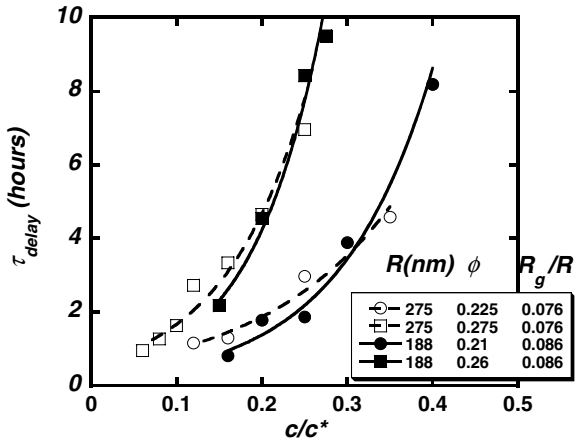

Figure 7. Delay time as a function of normalized polymer concentration for both particle radii at similar ϕ and R_g/R. The lines are exponential fits to the data.

decreasing R_g/R. Decreasing R_g/R also results in a stronger dependence of τ_{delay} on polymer concentration.

In addition to investigating the effects of R_g/R on delayed settling time, we are also interested in how particle size influences τ_{delay}. As noted above for the volume fractions studied here, independent of the precise value of $R_g/R(< 0.1)$, we found that delayed settling was not observed for particles with a radius of 100 nm. At these sizes, we only observed a slow settling regime with settling velocities that are an order of magnitude smaller than those observed for the 275 nm particle suspensions. This indicates a lower size cut-off, below which transient gel behaviour is not observable on practical timescales. The delay time is shown as a function of c/c^* for the two different particle radii samples of 188 and 275 nm at similar ϕ and R_g/R in figure 7. Transient gels for the 275 nm particles are first observed at smaller

polymer concentrations ($c/c^* \sim 0.10$–0.12) than for the 188 nm particles ($c/c^* \sim 0.14$–0.16). Physically, and based on theory [4–6, 11], we expect that at the same ϕ and R_g/R, localization will occur at the same c/c^*. Therefore we interpret this result as indicating the presence of residual van der Waals forces for the 275 nm particles that enhance the attractive forces between particles in the presence of depletion attractions and lead to a smaller c/c^* required for localization. The silica–decalin system has a small refractive index mismatch and hence van der Waals attractions between particles are not completely eliminated. At smaller particle radii (25–50 nm), the octadecyl coating on the silica particle surface has been shown to provide sufficient steric stabilization to mimic near-hard sphere behaviour in decalin [10]. However with increasing particle size, the attractive interaction is expected to get stronger.

Further evidence for attractions in the absence of polymer can be found in the sedimentation rates of the 188 and 275 nm colloids, providing a means to determine the particle size at which these attractions become significant. At volume fractions of 0.21 and 0.26, the 188 nm colloids have settling velocities of $u_{sed} = 0.0035$ cm h^{-1} ($\sim$10 nm s^{-1}) and 0.0025 cm h^{-1} ($\sim$7 nm s^{-1}), respectively. When divided by the settling velocity at this particle size at infinite dilution, u_0, this translates to $u_{sed}/u_0 \sim 0.36$ and $\sim$0.26, respectively. For the well characterized silica–cyclohexane hard sphere system, Kops-Werkhoven and Fijnaut [41] report $u_{sed}/u_0 \sim 0.22$–0.26 over a similar range of volume fractions, indicating that residual attractions in the 188 nm particles are weak enough to not significantly deviate from hard sphere settling. On the other hand, for the 275 nm colloid samples, $u_{sed}/u_0 \sim 0.57$ and 1.05 at volume fractions of 0.225 and 0.275, respectively, suggesting that the residual van der Waals attractions are indeed non-negligible at these particle sizes. Based on these sedimentation studies, we conclude that for the 188 nm particle samples near hard sphere behaviour can be achieved. However, residual attractions need to be taken into account in describing the behaviour of the 275 nm colloids.

Given the refractive indices of silica (1.448) and decalin (1.478), the Hamaker constant is estimated [42] to be $\sim 0.06 k_B T$ and the strength of attraction at contact (assumed to be a surface–surface separation of 1 nm) is $\sim 1 k_B T$. This corresponds to a contact value of a depletion potential generated at $c/c^* \sim 0.06$ when calculated according to the Asakura–Oosawa (AO) [43] model. If we assume that the well depth of the attractive van der Waals interactions can be described as corresponding to that induced between particles at a polymer concentration of $c/c^* = 0.06$, and that these residual attractions will lower the polymer concentration required to induce gelation, then the gelation polymer concentration for the 275 nm particles is lower than the value for the 188 nm particles which experience negligible residual attractions by an amount $c/c^* = 0.06$, i.e. $c_{gel}/c^*|_{275\ nm} \sim c_{gel}/c^*|_{188\ nm} - 0.06$. This assumption is supported by the mismatch in the gel boundary polymer concentrations as reported above.

For all of our subsequent analyses, we have used the adjusted polymer concentrations for the 275 nm particle samples by an addition of 0.06 to the actual polymer concentrations employed to account for the residual attractions in the system. In figure 8, we re-plot the data of figure 7 by using the adjusted polymer concentrations for the 275 nm particles. We emphasize that this method of adjusting the value of polymer concentrations to account for the presence of residual van der Waals attractions merely shifts the curves to the right and does not change their shape. As seen in figure 8, when keeping other parameters constant, a decrease in particle radius results in an increase in the time required to observe gel collapse. Also, τ_{delay} becomes more sensitive to polymer concentration and exhibits a stronger than linear dependence (the lines through the data points are exponential) for both particle sizes. Since the only difference in these experiments is the colloid radius, we propose that this distinction in τ_{delay} reflects the impact of gravity on setting the timescale for gel collapse.

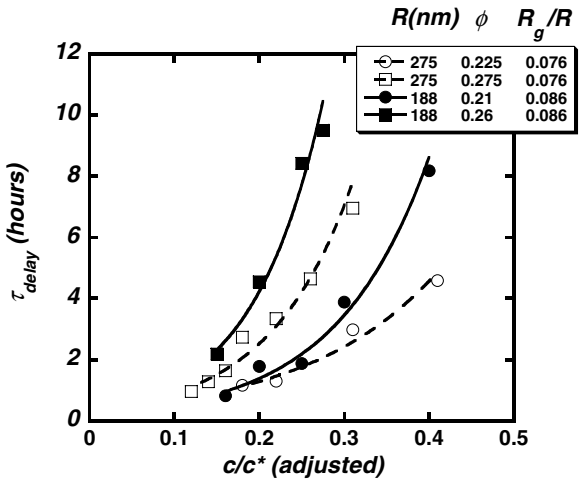

Figure 8. Delay time as a function of the adjusted normalized polymer concentration. The polymer concentrations for gels of the 275 nm particles have been adjusted to account for residual van der Waals attractions. The lines through the data are exponential fits. The data show that reducing the particle radius results in a stronger dependence of τ_{delay} on polymer concentration under similar conditions of ϕ and R_g/R.

5. Discussion

A large body of experimental [2, 9, 44–46] and theoretical work [4–8, 11, 28, 29] links the mechanical strength of colloidal depletion gels to volume fraction, ϕ, the range of attraction (R_g/R in our system), the strength of the attractive potential that physically bonds particles (c/c^* in our system), and the external perturbations that stress the gel network (gravity in our system). We have systematically probed the impact of each of the above factors on τ_{delay}. Our goal is to use these data to explore possible links between models of thermally activated particle motion and delayed settling. Our hypothesis is that rearrangements due to activated processes are the rate-limiting step in the catastrophic settling of depletion gels. We apply the activated barrier-hopping theory for depletion gels [23] to suggest a scaling relationship between the experimental τ_{delay} and the theoretical single particle barrier-hopping time, τ_{HOP}.

As seen in equation (2), parameters that have a significant impact on the barrier height, F_B, will have the greatest influence on the particle hopping times. Theoretical calculations of τ_{HOP}/τ_0 are shown as a function of polymer concentration, for a range of ϕ and two different values of R_g/R, in figure 9(a). In a manner similar to the experimental trends of τ_{delay}, τ_{HOP}/τ_0 increases with both ϕ and c/c^* for a given R_g/R. In addition, increasing R_g/R decreases τ_{HOP}/τ_0, which is qualitatively consistent with experimental observations. Figure 9(b) shows a master curve onto which all of the calculations in figure 9(a) roughly collapse by defining a composite parameter proposed by Chen *et al* [23], $\theta = G(\phi)[c/c^*][R/R_g]^{0.75}$. Here $G(\phi) = 0.5 + 7.8\phi + 27\phi^2$ is an empirical function used to collapse the theoretical data at different volume fractions, which also has a physical basis since it is closely related to the volume fraction dependence of the number of sticky depletion bonds per colloid as computed using PRISM theory [23]. The quality of the collapse is not as good for very low R_g/R values; however, this can be improved by modest changes to the exponent of R/R_g in the definition of θ. If the single particle events control delayed settling we anticipate that the delay times will also be controlled by the variable θ.

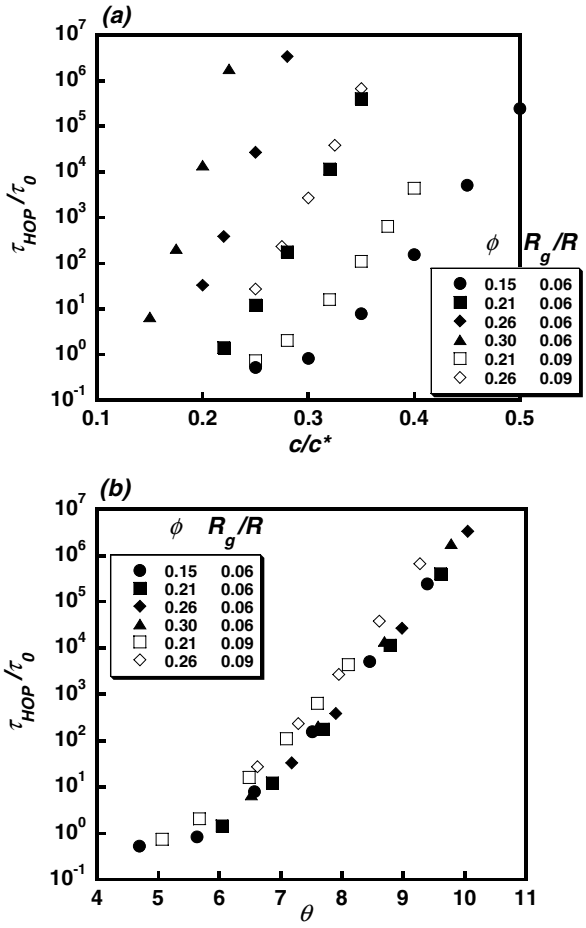

Figure 9. (a) Theoretical single particle hopping time [23] normalized to the elementary diffusion time as a function of c/c^* over a range of colloid volume fractions and for two values of R_g/R. (b) Dimensionless theoretical hopping time [23] as a function of the composite scaling variable $\theta = G(\phi)[c/c^*][R/R_g]^{0.75}$ for a range of c/c^*, ϕ and R_g/R values.

Figure 10 presents a log–linear plot of the experimental τ_{delay}/τ_0 data as a function of θ for different ϕ and R_g/R. The theoretically proposed [23] exponential scaling with θ captures the volume fraction, polymer concentration and R_g/R dependences reasonably well. Within experimental uncertainties, a master curve emerges for a given particle radius.

Hence, qualitatively, theory and experiments find an exponential scaling of τ_{HOP}/τ_0 and τ_{delay}/τ_0 with $\theta(\sim e^{a\theta})$. For the theory, the numerical prefactor $a \sim 4$, whereas from experiment $a \sim 0.45$ and ~ 0.30 for the 188 and 275 nm particles, respectively. The inset in figure 10 plots the data of the PMMA–decalin–polystyrene depletion system [12] in a manner suggested by theory [23]. These experiments were performed for colloids with $R = 301$ nm, $R_g/R \sim 0.06$ and increasing c/c^* for a range of volume fractions ($\phi = 0.15$–0.30). A similar collapse of the delay times is observed when plotted against the parameter θ. For this set of data, $a \sim 0.95$. For the two experimental systems, the numerical prefactors, a, are different from each other and the theoretical result. These differences highlight the possible role of specific characteristics of the experimental system, such as residual attractions, soft-core repulsions due

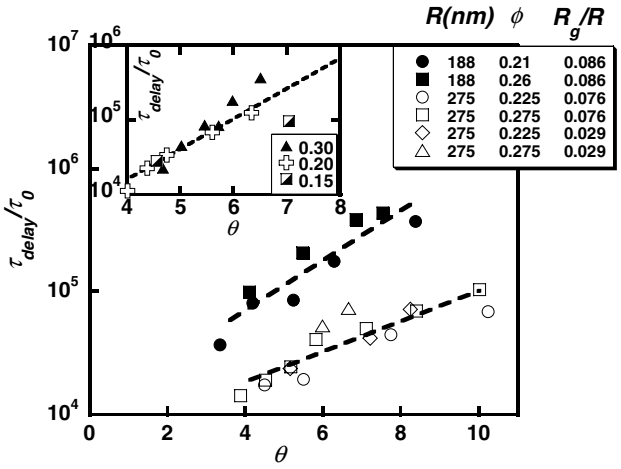

Figure 10. Log–linear plot of the experimental delay time normalized by the elementary Brownian diffusion time as a function of the parameter θ. The lines are exponential fits to the data. The collapse mimics that observed for single particle hopping times in figure 9(b). The data for gels of 188 nm particles is distinct from that of the 275 nm particles. The inset displays a similar collapse of the delay times for the PMMA colloid system [12].

to steric stabilization or variable gravitational stresses in modulating the dynamics of particle rearrangements. There is also the experimental issue of the role of vial diameter. We have not investigated this question, but comparison of our results with the measurements of Starr *et al* [47] suggests our vial size is greater than the so-called stress transmission length scale. We speculate the system-dependent physics not accounted for within the existing theoretical framework may be the primary origin of the discrepancies for the prefactor a. Of course, even more fundamental origins of the discrepancies of the disparate values of a cannot be ruled out. However, in spite of inherent complexities that regulate the exact dependences, the fact that the delay times for a wide range of c/c^*, ϕ and R_g/R values collapse reasonably well onto a master curve with θ as the scaling variable for two distinct experimental systems provides support for both the theory and the hypothesis that single-particle 'hopping' events are the rate-limiting step in determining the timescales for macroscopic gel collapse.

Although the absolute delay times for the different particle size samples are rather similar in magnitude, as seen in figure 8, we believe that the normalization by the elementary Brownian diffusion time, τ_0, is essential to capturing the particle-size-dependent physics that is independent of its trivial dependence on colloid radius. The presence of a particle size dependence in the collapse of the data in figure 10 clearly suggests additional effects associated with the absolute particle size are missing in the theory.

As rheological measurements on transient PMMA depletion gels [12] have demonstrated, increasing the external stress weakens the network strength and shortens $\tau_{\rm delay}$. The theory as currently applied does not incorporate the effects of gravitational stresses acting on non-density-matched particles. However, the theory has been recently generalized to include this aspect [28, 29]. The inset of figure 1 shows how external stress decreases the barrier, $F_{\rm B}$, thus enhancing mobility. Incorporating the gravitational stresses provides a framework for describing how an increase in the stress enhances bond-breakage rates, ultimately increasing the rate at which the gel structure coarsens, and reduces delay times. We note that enhanced bond breakage rates in the presence of a stress are also included in a model of Tanaka and co-workers [48].

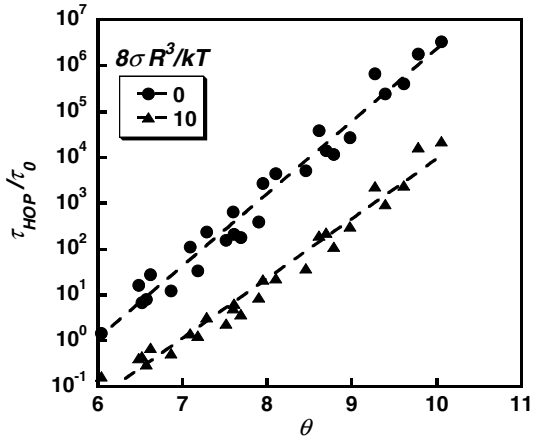

Figure 11. Dimensionless theoretical hopping time [23, 29] as a function of θ for two values of applied dimensionless stress, $8\sigma R^3/k_B T$. Predictions at different stresses collapse onto distinct master curves.

The predictions of the activated barrier-hopping theory in the presence of an external stress [28, 29] are shown in figure 11. At given values of ϕ, c/c^* and R_g/R (i.e. constant θ), increasing the forces acting on individual particles decreases τ_{HOP}/τ_0. However, the collapse of the τ_{HOP}/τ_0 predictions onto a master curve when plotted as a function of θ is retained under the influence of an external stress with a slightly smaller prefactor ($a \sim 3.75$). Within the context of the model, stress weakens particle localization, leading to faster 'hopping' times or larger bond breakage rates.

Since larger particles feel a stronger gravitational force, gels are subjected to a stronger stress when the colloid size increases. The enhanced gravitational force acting on gels composed of 275 nm particles, over those composed of 188 nm particles at a given θ, then provides a qualitative rationale for the collapse of τ_{delay} onto a single master curve for a given colloid size but different master curves for different particle sizes. In addition, large colloids exhibit a smaller elastic modulus and yield stress (all other factors being held constant), a trend which is also expected to result in enhanced gel collapsibility as particle radius increases.

Note that, within the theory, stress modifies the dependence of F_B on system parameters, giving rise to modestly different slopes of the master curves of τ_{HOP}/τ_0 as a function of θ. We obtain simple estimates of the magnitude of the gravitational forces on our particles based on two assumptions. The first is that the drag due to the up-flow of the solvent during the initial stages is negligible, and hence the only external force on the gel network is the gravitational force. The second is that, since the scattering studies of Shah *et al* [10] suggest that the percolated gel is composed of clusters of particles with radii that are ∼5–8 times the radius of the individual particles, we consider these clusters as the settling entities. The gravitational force is then $V_c \Delta\rho g$, where $V_c = \frac{4\pi}{3}(5-8R)^3 \sim (100-500)\frac{4\pi}{3}R^3$ is the volume of the cluster. Non-dimensionalizing the force by $(2R)/k_B T$, in a manner consistent with the theory, then gives non-dimensionalized forces of ∼10–50 for the 275 nm particles and ∼2–11 for the 188 nm particles. These numbers fall within the range of stress values for which the model predictions of hopping times in figure 11 display distinct universal curves. For the PMMA system in the inset of figure 10, $\Delta\rho \sim 300$ kg m^{-3} and $R = 301$ nm; employing the same cluster size, we obtained non-dimensionalized gravitational forces of ∼5–25. This range falls between that obtained for the 275 nm and the 188 nm particles. Indeed comparison of the inset

and main plot in figure 11 shows that the master curve for the PMMA colloids falls between the curves for our two silica systems. This seems qualitatively consistent with the rough estimates of the gravitational forces in the PMMA transient gels being intermediate between that for our 275 and 188 nm silica particles. However the origin of the differences in the slope or prefactor, a, in the relation $\tau_{\rm delay}/\tau_0 \sim {\rm e}^{a\theta}$ remains unclear.

A particle-size-dependent hopping time also provides a rationale for a lower particle-size cut-off below which we are unable to observe transient gel behaviour. At small particle sizes, longer hopping times and a steeper dependence on θ ensures that the window of polymer concentrations for the formation of transient gels is either very narrow or non-existent on the experimental timescale.

Finally, we comment on two very recent experimental studies of gel collapse by others [48, 49]. In contrast to our work, both these studies involved charged colloids at low volume fractions, where the concepts of percolation and fractal aggregate formation are important. In both studies the long time gel collapse phenomenon of present interest was not observed due to the very high interparticle attractions of the systems studied ($\sim 20 k_{\rm B}T$) and the unmeasurably long single particle activated hopping times. Manley *et al* [49] measured the 'creeping sedimentation' process, and found its characteristic timescale shortens with increasing (low) colloid volume fraction, opposite to our delayed gel collapse results. Tanaka *et al* [48] focused on the issue of coupling of phase separation and gel formation, including the idea that mechanical stress is induced in the gel via a viscoelastic mechanism which can generate network coarsening. This aspect has not been addressed in our theoretical analysis. However, the crucial point is that, in contrast to the recent studies [48, 49], our use of relatively weak depletion attractions results in experimentally relevant activated hopping timescales, which one might expect is the leading order process for triggering gel collapse.

6. Summary and conclusion

In this work we have conducted a systematic study of the delayed settling phenomenon in depletion gels using octadecyl silica particles. Our goal was to determine if there is a link between the delay times for gel collapse and the elementary barrier-crossing events predicted by the activated barrier-hopping theory [20, 23, 24, 27–29]. Building on observations made in the PMMA depletion system [12], we find that delayed settling is dependent on volume fraction, polymer concentration and ratio of polymer radius of gyration to particle radius. However, by suitably 'lumping' these variables into one composite parameter, θ, predicted to be the key scaling variable for the hopping time for gelled systems [23], the delay times for a given particle size collapse reasonably well onto master curves for two distinct experimental systems (PMMA and silica depletion gels). The theoretical calculations predict a steeper dependence of hopping times on θ than is observed for the delay times in the two distinct experimental systems. This might be attributable to subtle (and unaccounted for) features of system-dependent particle interactions that modulate the dynamics of particle rearrangements. However, more theoretical work is clearly required to better understand this quantitative aspect. Nevertheless, we find it rather remarkable that despite the multitude of complex macroscopic structural evolutions observed in transient gels prior to delayed settling, a successful scaling and collapse of delay times can be achieved. This provides significant support for the idea that the underlying physical processes giving rise to gel collapse are tightly coupled to single particle activated hopping events. The master curves are observed to be dependent on the particle radius, and this trend can be qualitatively accounted for by the difference in gravitational force acting on particles of different sizes.

Acknowledgments

The authors thank Professor M Fuchs for access to the code for predicting $S(q)$. KSS thanks Wilson Poon for a helpful discussion. We would also like to thank Dr Y L Chen for his insights into the theory calculations. This work is supported by the US Department of Energy, Division of Materials Sciences, under award No DEFG02-91ER45439, through the Frederick Seitz Materials Research Laboratory at the University of Illinois at Urbana-Champaign. Scanning electron microscopy measurements for this work were carried out in the Center for Microanalysis of Materials, University of Illinois at Urbana-Champaign, which is partially supported by the US Department of Energy under grant DEFG02-91-ER45439

References

[1] Larson R G 1999 *The Structure and Rheology of Complex Fluids* (New York: Oxford University Press)
[2] Prasad V, Trappe V, Dinsmore A D, Segre P N, Cipelletti L and Weitz D A 2003 *Faraday Discuss.* **123** 1
[3] Poon W C K 2002 *J. Phys.: Condens. Matter* **14** R859
[4] Bergenholtz J and Fuchs M 1999 *Phys. Rev.* E **59** 5706
[5] Bergenholtz J, Poon W C K and Fuchs M 2003 *Langmuir* **19** 4493
[6] Dawson K, Foffi G, Fuchs M, Gotze W, Sciortino F, Sperl M, Tartaglia P, Voigtmann T and Zaccarelli E 2001 *Phys. Rev.* E **63** 011401
[7] Fabbian L, Gotze W, Sciortino F, Tartaglia P and Thiery F 1999 *Phys. Rev.* E **59** R1347
[8] Zaccarelli E, Foffi G, Dawson K A, Sciortino F and Tartaglia P 2001 *Phys. Rev.* E **63** 031501
[9] Shah S A, Chen Y L, Schweizer K S and Zukoski C F 2003 *J. Chem. Phys.* **119** 8747
[10] Shah S A, Chen Y L, Ramakrishnan S, Schweizer K S and Zukoski C F 2003 *J. Phys.: Condens. Matter* **15** 4751
[11] Chen Y L and Schweizer K S 2004 *J. Chem. Phys.* **120** 7212
[12] Poon W C K, Starrs L, Meeker S P, Moussaid A, Evans R M L, Pusey P N and Robins M M 1999 *Faraday Discuss.* **112** 143
[13] Kilfoil M L, Pashkovski E E, Masters J A and Weitz D A 2003 *Phil. Trans. R. Soc.* A **361** 753
[14] Allain C, Cloitre M and Wafra M 1995 *Phys. Rev. Lett.* **74** 1478
[15] Parker A, Gunning P A, Ng K and Robins M M 1995 *Food Hydrocolloids* **9** 333
[16] Glasrud G G, Navarrete R C, Scriven L E and Macosko C W 1993 *AIChE J.* **39** 560
[17] Zaccarelli E, Foffi G, Sciortino F and Tartaglia P 2003 *Phys. Rev. Lett.* **91** 108301
[18] Solomon M J and Varadan P 2001 *Phys. Rev.* E **63** 051402
[19] Bissig H, Romer S, Cipelletti L, Trappe V and Schurtenberger P 2003 *Phys. Chem. Commun.* **6** 21
[20] Schweizer K S and Saltzman E J 2003 *J. Chem. Phys.* **119** 1181
[21] Kirkpatrick T R and Wolynes P G 1987 *Phys. Rev.* A **35** 3072
[22] Gotze W 1999 *J. Phys.: Condens. Matter* **11** A1
[23] Chen Y L, Kobelev V and Schweizer K S 2005 *Phys. Rev.* E **71** 041405
[24] Schweizer K S 2005 *J. Chem. Phys.* **123** 244501
[25] Fuchs M and Schweizer K S 2002 *J. Phys.: Condens. Matter* **14** R239
[26] Kramers H A 1940 *Physica* **7** 284
[27] Kobelev V and Schweizer K S 2005 *Phys. Rev.* E **71** 021401
[28] Kobelev V and Schweizer K S 2005 *J. Chem. Phys.* **123** 164902
[29] Kobelev V and Schweizer K S 2005 *J. Chem. Phys.* **123** 164903
[30] Stober W, Fink A and Bohn E 1968 *J. Colloid Interface Sci.* **26** 62
[31] Bogush G H, Tracy M A and Zukoski C F 1988 *J. Non-Cryst. Solids* **104** 95
[32] Van Helden A K, Jansen J W and Vrij A 1981 *J. Colloid Interface Sci.* **81** 354
[33] Shah S A, Chen Y L, Schweizer K S and Zukoski C F 2003 *J. Chem. Phys.* **118** 3350
[34] Segre P N, Prasad V, Schofield A B and Weitz D A 2001 *Phys. Rev. Lett.* **86** 6042
[35] Poon W C K, Pirie A D and Pusey P N 1995 *Faraday Discuss.* **101** 65
[36] Buscall R and White L R 1987 *J. Chem. Soc. Faraday Trans.* **83** 873
[37] Happel J and Brenner H 1973 *Low Reynolds Number Hydrodynamics* (Leyden: Noordhoff International Publishing)
[38] Channell G M and Zukoski C F 1997 *AIChE J.* **43** 1700
[39] Evans R M L and Starrs L 2002 *J. Phys.: Condens. Matter* **14** 2507
[40] Lekkerkerker H N W, Poon W C K, Pusey P N, Stroobants A and Warren P B 1992 *Europhys. Lett.* **20** 559

[41] Kops-Werkhoven M M and Fijnaut H M 1982 *J. Chem. Phys.* **77** 2242
[42] Russel W B, Saville D A and Schowalter W R 1989 *Colloidal Dispersions* (Cambridge: Cambridge University Press)
[43] Asakura S and Oosawa F 1958 *J. Polym. Sci.* **33** 183
[44] Grant M C and Russel W B 1993 *Phys. Rev.* E **47** 2606
[45] Rueb C J and Zukoski C F 1997 *J. Rheol.* **41** 197
[46] Ramakrishnan S, Gopalakrishnan V and Zukoski C F 2005 *Langmuir* **21** 9917
[47] Starrs L, Poon W C K, Hibberd D J and Robins M M 2002 *J. Phys.: Condens. Matter* **14** 2485
[48] Tanaka H, Nishikawa Y and Koyama T 2005 *J. Phys.: Condens. Matter* **17** L143–53
[49] Manley S, Skotheim J M, Mahadevan L and Weitz D A 2005 *Phys. Rev. Lett.* **94** 218302